

Lab on a Chip

Accepted Manuscript



This is an *Accepted Manuscript*, which has been through the Royal Society of Chemistry peer review process and has been accepted for publication.

Accepted Manuscripts are published online shortly after acceptance, before technical editing, formatting and proof reading. Using this free service, authors can make their results available to the community, in citable form, before we publish the edited article. We will replace this *Accepted Manuscript* with the edited and formatted *Advance Article* as soon as it is available.

You can find more information about *Accepted Manuscripts* in the [Information for Authors](#).

Please note that technical editing may introduce minor changes to the text and/or graphics, which may alter content. The journal's standard [Terms & Conditions](#) and the [Ethical guidelines](#) still apply. In no event shall the Royal Society of Chemistry be held responsible for any errors or omissions in this *Accepted Manuscript* or any consequences arising from the use of any information it contains.

ARTICLE

A microfluidic device and automatic counting system for the study of *C. elegans* reproductive aging

Siran Li,^{1,2} Howard A. Stone³ and Coleen T. Murphy^{1,4,*}

¹Lewis-Sigler Institute for integrative Genomics, Princeton University, Princeton, NJ 08544, USA

Departments of ²Electrical Engineering, ³Mechanical and Aerospace Engineering and ⁴Molecular Biology, Princeton University, Princeton, NJ 08544, USA

Summary

The nematode *Caenorhabditis elegans* (*C. elegans*) is an excellent model to study reproductive aging because of its short life span, its cessation of reproduction in mid-adulthood, and the strong conservation of pathways that regulate longevity. During its lifetime, a wild-type *C. elegans* hermaphrodite usually lays about 200-300 self-fertilized hatchable eggs, which mainly occurs in the first three to five days of adulthood. Here, we report the development of a microfluidic assay and a real-time, automatic progeny counting system that records progeny counting information from many individual *C. elegans* hermaphrodites. This system offers many advantages compared to conventional plate assays. The flow of non-proliferating bacteria not only feeds the worms but also flushes the just-hatched young progeny through a filter that separates mothers from their offspring. The progeny that are flushed out of the chamber are detected and recorded using a novel algorithm. In our current design, one device contains as many as 16 individual chambers. Here we show examples of real-time progeny production information from wild-type (N2) and *daf-2* (insulin receptor) mutants. We believe that this system has the potential to become a powerful, high time-resolution tool to study the detailed reproduction of *C. elegans*.

Introduction

The decline in female reproductive ability, which is one of the earliest aging phenotypes that human beings experience, is not well understood. For women over 35 years of age, there is a rapidly rising risk of infertility, birth defects, and miscarriage, due to age-related decline of oocyte quality.¹ The cause of this

decline remains elusive, but is likely to be genetically regulated. Therefore, the ability to identify genetic regulators of reproductive aging is an important goal for human health.

Caenorhabditis elegans (*C. elegans*) is a good model to study reproductive aging for two main reasons. First, *C. elegans* has a short life span and an even shorter reproductive span, with a post-reproductive lifespan that is proportionately similar to that of women. A wild-type worm raised on agar plates usually lives for 2-3 weeks but ceases reproduction between Day 3 and Day 6 of adulthood.²⁻⁴ Second, similar to human females, the reproductive ability of *C. elegans* also is limited by oocyte quality.⁵ More than 80% of worm proteins have human orthologs⁶, and many longevity regulatory mechanisms are evolutionarily conserved⁷, suggesting that identifying regulators of reproductive aging in *C. elegans* will be relevant for understanding and regulation of human reproductive aging. We and others have developed *C. elegans* as a model to study reproductive aging^{2,5}, and we have found that the TGF- β signalling pathway⁴, the insulin/IGF-1 signalling pathway^{2,4,5}, and the caloric restriction pathway^{4,8} all regulate the reproductive aging process, although the former is specific to reproduction, while the latter two regulate both reproductive aging and longevity.

However, for reproductive aging studies of *C. elegans*, it is difficult to record and analyze the number and timing of the laying of fertilized eggs. In conventional reproductive aging studies that are performed on 35 mm single-well agar plates or 12-well plates, researchers must transfer individual worms daily to a new plate and manually count the number of progeny that have hatched on the old plate after several days⁵. This procedure is inconvenient and labor-intensive. Furthermore, since the time resolution is at the level of one day and the reproductive span of wild-type *C. elegans* is usually 3-5 days, to achieve statistically significant results, it is necessary to pick at least 40 worms per strain at the beginning of the experiment. As a result, this plate assay not only has low time resolution, but is also labor-intensive.

In the past ten years, microfluidic technologies have provided new tools for *C. elegans* research.⁹ In particular, fluidic chambers can be micro-fabricated to confine and guide the worm's movement and to conduct on-line or off-line analyses. These microfluidic methods have advantages over plate assays in many applications, for example, immobilizing worms for imaging or laser ablation¹⁰⁻¹⁶, analyzing *C. elegans*' response or behavior when exposed to different chemicals or bacteria¹⁷⁻¹⁸, worm sorting and screening¹⁹⁻²³, and long-term liquid culture for aging studies²⁴⁻²⁶, as well as other investigations²⁷⁻²⁹.

Here, we report the development of a high time-resolution, automatic *C. elegans* progeny counting system that is based on microfluidic methods and a simple optical setup. This system, with a single hermaphrodite in a single microfluidic chamber throughout its reproductive period, can automatically detect and count in

real time every progeny in its L1 stage (first larval stage, just after hatching from eggs) from each hermaphrodite mother. Using this experimental system, we obtain progeny production frequency and progeny profile information. Our method reveals valuable progeny information that cannot be collected easily in conventional plate assays, and provides researchers a new way to compare the reproductive spans of different *C. elegans* mutants, which will be important in developing high-throughput methods for the genetic analyses of reproductive aging regulation.

Results

Reproductive microfluidic device design

We have designed a microfluidic device with chambers for individual worms, aligned in parallel for straightforward monitoring by a camera connected to a computer. **Figure 1a** illustrates the layout of our microfluidic device, which has 16 chambers for 16 worms, symmetrically designed with eight chambers on each side and separately connected to a wide main channel. This design serves three purposes. First, it simplifies the loading of worms into each chamber. Second, the main channel functions as a transport pipeline of bacteria for feeding the worms. Third, the main flow also serves as a driving force to push progeny out of the chamber into a serpentine channel immediately after they are hatched from fertilized eggs. Connecting the main channel and each individual chamber is a short narrow channel that only allows one L4 stage worm to stay in temporarily during the loading step.

When all eight worms are aligned in these channels, they are pushed into their individual chambers simultaneously using higher pressure and they remain in these chambers throughout the experiment. There is a 10 μm -high base at the end of every narrow channel that allows for large deformation while loading the worms with high pressure¹⁸, and also provides a wide passage for the main flow to flush the progeny out of the chambers. A high magnification image is shown in **Figure S1**. A critical feature of this device is a filter located in the bottom of each chamber that separates the mother hermaphrodites and the progeny, as shown in **Figure 1b**. The channels of the filter are 20 μm wide, which only allow L1 worms to pass through and retains all unhatched eggs, unfertilized oocytes, and the mother inside the chamber. These L1-stage worms quickly pass through the serpentine channels and enter directly into the downstream sixteen straight channels that are arranged in parallel to each other to allow simultaneous monitoring. The channels cover a 2 mm x 2 mm area defined as “the counting region”. **Figure 2** shows an optical image of the counting region and the schematic of the automatic progeny counting system.

Device fabrication

The microfluidic device was fabricated using standard soft lithography. SU-8 2015 and SU-8 2075 were spin-coated on a wafer to the thickness of 10 μm and 60 μm , respectively. The mold surface was treated with 1,1,2,2-tetrahydrooctyl-1-trichlorosilane to facilitate the release of the PDMS from the mold. The mixed PDMS solution (10:1 ratio) was poured on the surface of the mold to obtain a 1 cm thick layer after baking. After peeling the PDMS layer off the mold, holes were punched in the PDMS to define inlets and outlets. Oxygen plasma was used to treat the surface of the PDMS and a piece of glass slide before they were bonded together. Immediately after bonding, 5% Pluronic F127 solution was flowed through the device and held for 30 minutes¹⁷. This surfactant forms a long-term monolayer on the surface of both the PDMS and the glass and thus prevents attachment of bacteria¹⁷. Finally, the device was washed with S-basal buffer.

Worm loading and liquid culture

Worms are maintained on NGM plates³⁰. We placed 20 L4 worms per strain onto a new NGM plate. After 10 hours, these worms were in their late L4 stage and no eggs were visible on the plate. The worms were washed off the plate with S-basal buffer and about 10 worms were drawn into a syringe. We inserted the syringe tubing in the inlet, connected another syringe to the temporary side-inlet, and with the resulting flow, eight worms were aligned in the narrow channels, while the superfluous worms, if any, remained in one of the two syringes. After these eight worms were in position, a pulse of high pressure was applied by a syringe to push the worms into their individual chambers, and then the side-inlet was closed by a solid steel plug.

UV-killed bacteria were used to prevent live bacterial proliferation that might potentially form biofilms³¹ and block the filters and the channels. Each day, after an inoculation was grown overnight, fresh OP50 bacteria was exposed to ultra-violet light in a Syngene Ingenius gel box for 40 minutes to kill the bacteria. The final concentration of the bacteria solution flowed into the device was 10^9 cells per mL in the S-basal solution, previously tested in a microfluidic life-span assay²⁴. The concentration of the bacteria was measured by a Nanodrop 2000C (Thermo Scientific). Tween 20 detergent solution was used to further reduce the chance of dead bacteria clogging the device. A syringe with the solution of bacteria then replaced the previous worm-loading syringe. This solution contained non-proliferating OP50 bacteria in S-basal buffer with 1×10^{-4} (v/v) Tween 20 detergent. A syringe pump was used to generate the bacteria/buffer flow. Instead of running the syringe pump continuously, we ran the device 3.3 minutes and paused for 10 minutes with an average flow rate of 2 $\mu\text{L}/\text{min}$, in order to reduce the mechanical stress on

the worms caused by the laminar flow. Images of a hermaphrodite *C. elegans* in its chamber on different days are shown in **Figure S2**.

Automatic counting and data recording

As discussed above, the counting region that contains 16 parallel channels is designed to capture newly-hatched L1 worms flowing through the channels with high optical resolution, while imaging as many channels in a frame as possible. Each channel is 60 μm wide, 800 μm long and the space in between is 60 μm . This counting region is captured through a stereo microscope with a Basler CMOS camera controlled by the Laboratory Virtual Instrument Engineering Workbench (LabVIEW). Although fluorescent tracking is also an option, for the purpose of wide application of this approach, the system is not based on fluorescence imaging to avoid dependence on fluorescent markers. The schematic of the imaging and counting system is shown in **Figure 2a**. We determined that for the flow rates we used, a frame rate of 3.75 frames per second was sufficient to guarantee that a worm is captured at least once while flowing through the counting area. The program counts every moving worm in real time, and saves the time point and the channel number information so that it is not necessary to save large video files for later image analysis.

In order to process the images, we first tried to use the average intensity of a frame to judge whether a worm was present. We used the average intensity in the blue rectangle shown in **Figure 2b** and subtracted the average intensity in the red rectangle representing the background of a frame, and so determined the final average intensity of a channel, which we report in **Figure 3a**. From the results shown in Figure 3a we can see that the baseline intensity recorded from each channel was not only different from each other in level but drifted over time. As a result, it was difficult to set a threshold to extract the signal representing the presence of a worm. Therefore, we developed a counting algorithm to extract the worm signal from the background. We defined it as the “standard deviation” signal, as depicted by equation (1), where the $Intensity_k$ is the standard deviation intensity of the k -th channel area (in blue). As shown in **Figure 3b**, we used the a_k ($k = 1, 2, 3, \dots, 16$) array to save the previous average intensity of each pixel in each of the 16 channel regions. The *Background* array b saved the pixel intensity for the current image. Let c_k represent the pixel intensity of the k -th channel in the present image and define I_k as the “standard deviation” signal of the k -th channel

$$I_k = \frac{1}{n*m} \sum_{i,j} (c_k(i,j) - b(i,j) - a_k(i,j))^2 \quad (1)$$

After every image, we renew a_k by:

$$a_k(i,j)_{new} = 0.99 * a_k(i,j) + 0.01 * (c_k(i,j) - b(i,j)) \quad (2)$$

Basically, a_k was updated every time by weighting 1% on the current frame and 99% on the original value. There are two considerations behind this updating logic. First, as time goes by, the intensity of the counting area gradually changes, though very slightly. Therefore, we need to update a_k to reflect this change in the background. We feel that 1% weight on the new frame is appropriate in this updating algorithm because the intensity of some pixels in this counting area will increase dramatically when a worm passes through the counting area (most of the time, there is no worm in the counting area). So we do not want a_k to change a lot in this case since a_k is intended to measure the background of the counting area. In a word, a_k was designed in the form of equation (2) to reflect the slow long-term intensity change in each counting area without any effect from a sudden, random intensity shock from a certain frame.

With this approach, as illustrated in the results shown in **Figure 3b**, we find that the baselines are about the same magnitude and that there are many distinct peaks above the baseline. We took a video and compared the worm frame with the standard deviation value we defined, and we found that all of the peaks were actual worm signals and all the worm signals were marked by the peaks (see the supplementary information **Figure S4**, **Table S1** and **Video S1**.) Therefore, we determined that with these steps the signal intensity between 8 and 40 represented worm signals and are identified by a program written in Matlab, as shown in **Figure 3d-e**. Because every worm appears in the counting region at least once, this program also has the ability to recognize several consecutive standard deviation values within a certain range as a single worm signal instead of signals from multiple worms.

Reproductive span of wild-type worms and long-lived *daf-2* worms

DAF-2 is the only known *C. elegans* insulin pathway receptor⁵. In the *daf-2* mutant background, reduction of the insulin pathway signalling reduces the AKT-dependent phosphorylation of DAF-16, causing the DAF-16 protein to enter into the nucleus and extending both lifespan and reproductive span^{2,4,5,8,32}. To test the function of the device and our automatic counting system, we compared the reproductive spans of wild-type (N2) worms and long-lived *daf-2* mutants on standard reproductive span assay plates and in our device. We obtained the worm signals from the standard deviation peaks as indicated above, and also verified these signals using the corresponding saved images. Based on this information, we plot all of the time points at which progeny pass through the channel. For example, **Figure 4a** shows the progeny information from four N2 worms and four *daf-2* mutant worms, where a peak represents a progeny that has been extracted and confirmed from the “standard deviation” information. **Table S2** shows the progeny number every 4 hours of the eight worms in Figure 4a. All the worms’ progeny traces are shown in **Figure S5**. The last progeny time-points give us all of the information necessary to plot the reproductive span curve of a strain, as shown in **Figure 4b**.

The conventional plate-based approach is very labor-intensive, and has a low time-resolution at the level of one day (see **Figure 4c**). For the conventional self-reproductive span on a plate, we usually pick at least 48 worms per strain at the beginning of the assay and place each worm on a single agar plate. Unlike the reproductive span assays we measure with our microfluidic device, there are usually only 4-6 time points for the conventional reproductive span curve, so we need more than 40 worms to obtain statistically significant results. These worms need to be transferred from the original plate onto a new plate every day, and the original plates are checked two days later for hatched progeny. However, with our automatic counting microfluidic system, given the high frame rate and the measurement approach, the time resolution of our system is at the second to minute level. As shown by the results in **Figure 4b**, 13 N2 and 15 *daf-2* worms are sufficient to distinguish the reproductive spans of N2 and *daf-2* in the device with statistical significance (Mean RS \pm SD = 4.70 \pm 0.28 days for N2, 6.63 \pm 0.50 days for *daf-2*, $p = 0.001$). Similar to findings observed using traditional plate assays (Mean RS \pm SD = 3.98 \pm 0.15 days for N2, 5.52 \pm 0.20 days for *daf-2*, $p < 0.0001$), the *daf-2* mutants have a 40% longer reproductive span than N2 worms^{4,5}.

The progeny profiles of N2 and *daf-2*

We found that the N2 and *daf-2* worms have different progeny profiles over the reproductive period. For example, we measured the progeny number distribution every eight hours for more than 9 days of different genotypes in the microfluidic devices, as shown by the results presented in **Figure 5**. *daf-2* mutants have a longer reproductive period than wild type, while N2's reproduction is concentrated in the first three days, as was previously shown². Thus, our system can provide researchers with an easy way to record the progeny number and the timing of progeny production, allowing more detailed studies with less manual labor.

Conclusions

We have developed a microfluidic automatic counting system to record the progeny production of *C. elegans*. This device separates progeny from their mothers, and our image analysis algorithm counts progeny in real time. We developed a new method for automatically counting moving *C. elegans* in different regions of the device, which can be extended to detecting other kinds of moving objects or organisms. We also showed that using this system, we successfully conducted a reproductive span assay of

the wild-type worm N2 and the *daf-2* mutant in the device, and obtained the time course of progeny production. This approach provides much more information than does the conventional plate assay for reproductive aging studies, and will allow new opportunities to compare mutants with different progeny profiles. The high time resolution of this assay will allow researchers to identify mutants with slight extensions of the reproductive span, and can potentially be combined with other optical manipulation and interrogation methods. With the simple optical set-up, the throughput can be further improved for high-throughput screens.

Acknowledgements

We thank W. Keyes for assistance, and N. Pegard and members of the Murphy lab for helpful discussion. We also thank the *Caenorhabditis* Genetics Center for strains, Princeton Micro/Nano fabrication laboratory (MNFL) and Princeton microfluidics laboratory for equipment maintenance. This work was supported by an NIH innovator award (DP2OD004402) to C.T.M.

Notes and references

- 1 E. R. te Velde and P. L. Pearson. *Human Reproduction Update*, 2002, **8**, 141-154.
- 2 S. E. Hughes, K. Evason, C. Xiong, K. Kornfeld, *PLoS Genetics*, 2007, **3**, e25.
- 3 S. Andux, and R. E. Ellis. *PLoS Genetics*, 2008, **4**, e1000295.
- 4 S. Luo, W. M. Shaw, J. Ashraf, and C. T. Murphy. *PLoS Genetics*, 2009, **5**, e1000789.
- 5 S. Luo, G. A. Kleemann, J. M. Ashraf, W. M. Shaw, and C. T. Murphy. *Cell*, 2010, **143**, 299-312.
- 6 C. Lai, C. Chou, L. Ch'ang, C. Liu, and W. Lin. *Genome Research*, 2000, **10**, 703-713.
- 7 C. Kenyon, *Cell*, 2005, **120**, 449-460.
- 8 C. Huang, C. Xiong, and K. Kornfeld, *Proceedings of the National Academy of Sciences*, 2004, **101**, 8084-8089.
- 9 N. A. Bakhtina and J. G. Korvink. *RSC Advances*, 2014, **4**, 4691-4709.
- 10 K. Chung and H Lu. *Lab on a Chip*, 2009, **9**, 2764-2766.
- 11 C. Samara, C. B. Rohde, C. L. Gilleland, S. Norton, S. J. Haggarty and M. F. Yanik, *Proceedings of the National Academy of Sciences*, 2010, **107**, 18342-18347.
- 12 C. L. Gilleland, C. B. Rohde, F. Zeng and M. F. Yanik, *Nature Protocols*, 2010, **5**, 1888-1902.
- 13 F. Zeng, C. B. Rohde and M. F. Yanik, *Lab on a Chip*, 2008, **8**, 653-656.
- 14 J. Krajniak and H. Lu. *Lab on a Chip*, 2010, **10**, 1862-1868.
- 15 P. B. Allen, A. E. Sgro, D. L. Chao, B. E. Doepker, J. S. Edgar, K. Shen and D. T. Chiu. *Journal of Neuroscience Methods*, 2008, **173**, 20-26.

- 16 S. E. Hulme, S. S. Shevkoplyas, J. Apfeld, W. Fontana and G. M. Whitesides, *Lab on a Chip*, 2007, **7**, 1515-1523.
- 17 D. R. Albrecht and C. I. Bargmann, *Nature Methods*, 2011, **8**, 599-605.
- 18 K. Chung, M. Zhan, J. Srinivasan, P. W. Sternberg, E. Gong, F. C. Schroeder and H. Lu, *Lab on a Chip*, 2011, **11**, 3689-3697.
- 19 C. B. Rohde, F. Zeng, R. Gonzalez-Rubio, M. Angel and M. F. Yanik, *Proceedings of the National Academy of Sciences*, 2007, **104**, 13891-13895.
- 20 P. Rezai, S. Salam, P. R. Selvaganapathy and B. P. Gupta, *Lab on a Chip*, 2012, **12**, 1831-1840.
- 21 K. Chung, M. M. Crane and H. Lu, *Nature Methods*, 2008, **5**, 637-643.
- 22 S. R. Lockery, S. E. Hulme, W. M. Roberts, K. J. Robinson, A. Laromaine, T. H. Lindsay, G. M. Whitesides and J. C. Weeks, *Lab on a Chip*, 2012, **12**, 2211-2220.
- 23 P. Rezai, A. Siddiqui, P. R. Selvaganapathy and B. P. Gupta, *Lab on a Chip*, 2010, **10**, 220-226.
- 24 S. E. Hulme, S. S. Shevkoplyas, A. P. McGuigan, J. Apfeld, W. Fontana and G. M. Whitesides, *Lab on a Chip*, 2010, **10**, 589-597.
- 25 H. Wen, W. Shi and J. Qin, *Biomedical Microdevices*, 2012, **14**, 721-728.
- 26 B. Xian, J. Shen, W. Chen, N. Sun, N. Qiao, D. Jiang and T. Yu, *Aging Cell*, 2013, **12**, 398-409.
- 27 H. Chuang, D. M. Raizen, A. Lamb, N. Dabbish and H. H. Bau, *Lab on a Chip*, 2011, **11**, 599-604.
- 28 H. Ma, L. Jiang, W. Shi, J. Qin and B. Lin, *Biomicrofluidics*, 2009, **3**, 044114.
- 29 J. Yang, Z. Chen, P. Ching, Q. Shi and X. Li, *Lab on a Chip*, 2013, **13**, 3373-3382.
- 30 S. Brenner, *Genetics*, 1974, **77**, 71-94
- 31 K. Drescher, Y. Shen, B. L. Bassler and H. A. Stone, *Proceedings of the National Academy of Sciences*, 2013, **110**, 4345-4350.
- 32 K. Lin, H. Hsin, N. Libina and C. Kenyon. *Nature Genetics*, 2001, **28**, 139-145.

Figures

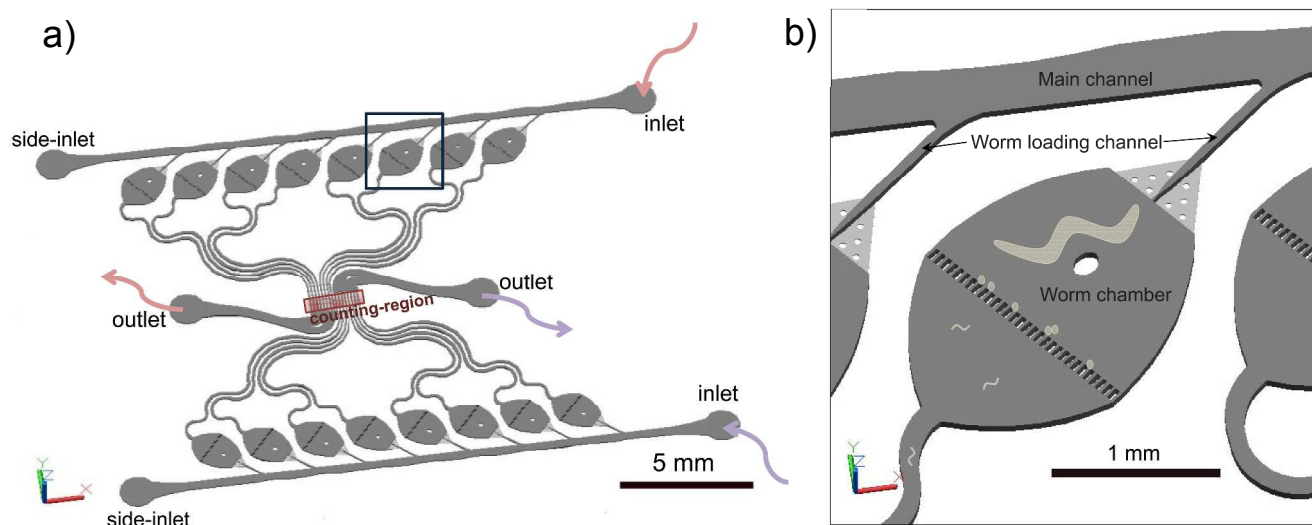


Figure 1: Schematic of the microfluidic device. **a)** A sketch of the microfluidic device with the symmetrical design of 8 chambers on each side. The inlets and side-inlets are used for loading of worms and the inlets and the outlets are used for the flow of bacteria. The counting region in the middle of the device is about 2 mm x 2 mm for camera monitoring (red rectangle). **b)** Enlarged image of a single chamber. There is a 1 mm long narrow channel and a 10 μm wide base (light color). The main chamber has a 20 μm wide filter to separate the progeny from the mothers.

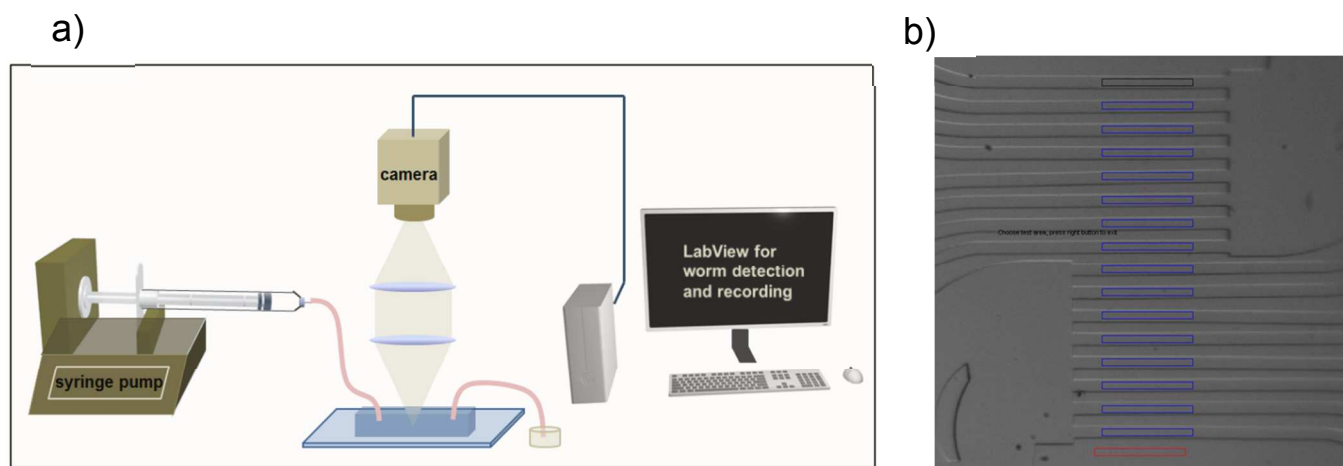
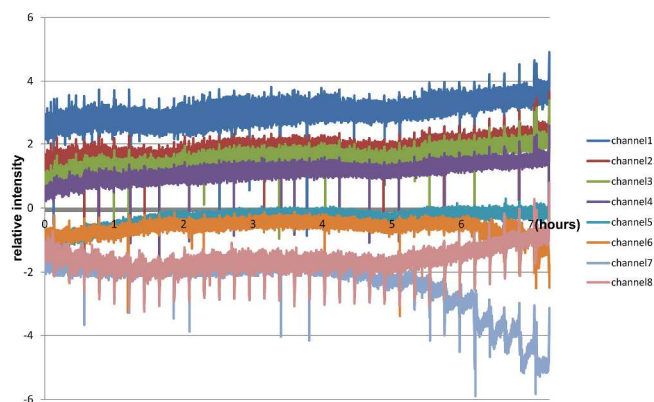
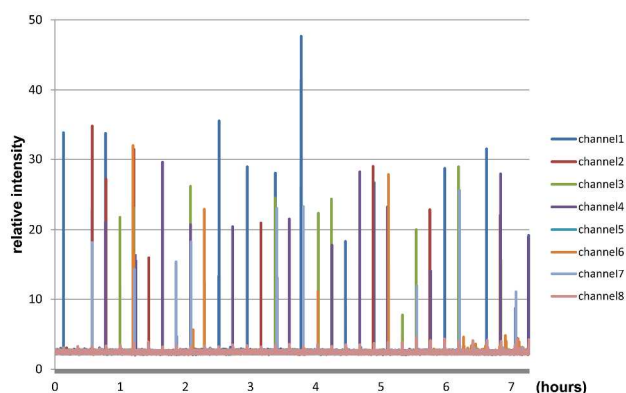


Figure 2: The worm counting system. **a)** The schematic of the automatic progeny counting system. A syringe pump flushes the progeny through the counting region, where they are imaged by a CMOS camera and recorded and analysed by LabVIEW and Matlab. **b)** An optical image shows the counting region. After we define three reference points (as shown in **Figure S3**), the black and blue rectangles are drawn automatically as the worm counting regions for each channel. The red rectangle is the reference background region for image analysis. The 16 blue or black regions and the red background region are of the same size.

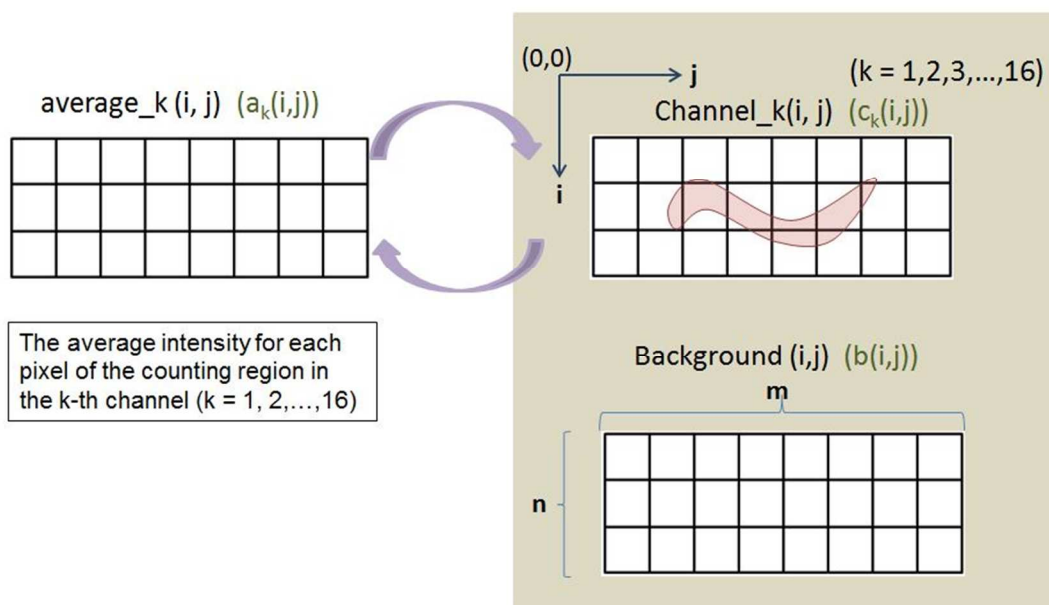
a)



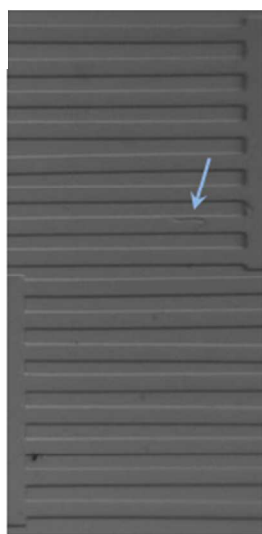
b)



c)



d)



e)

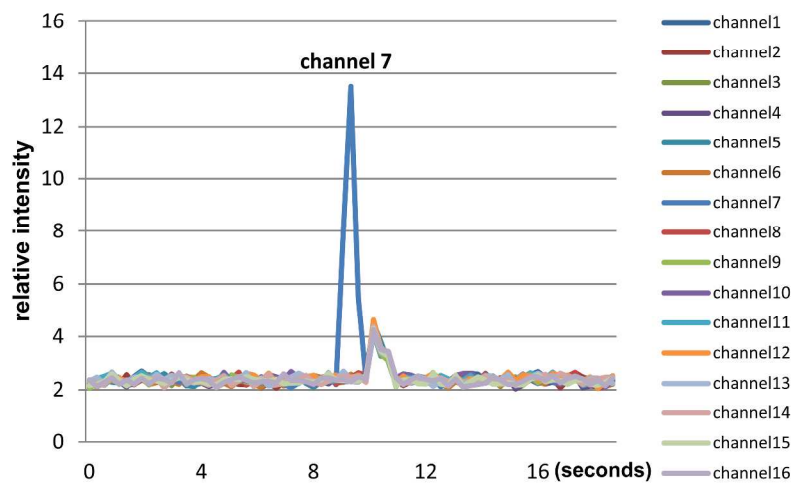
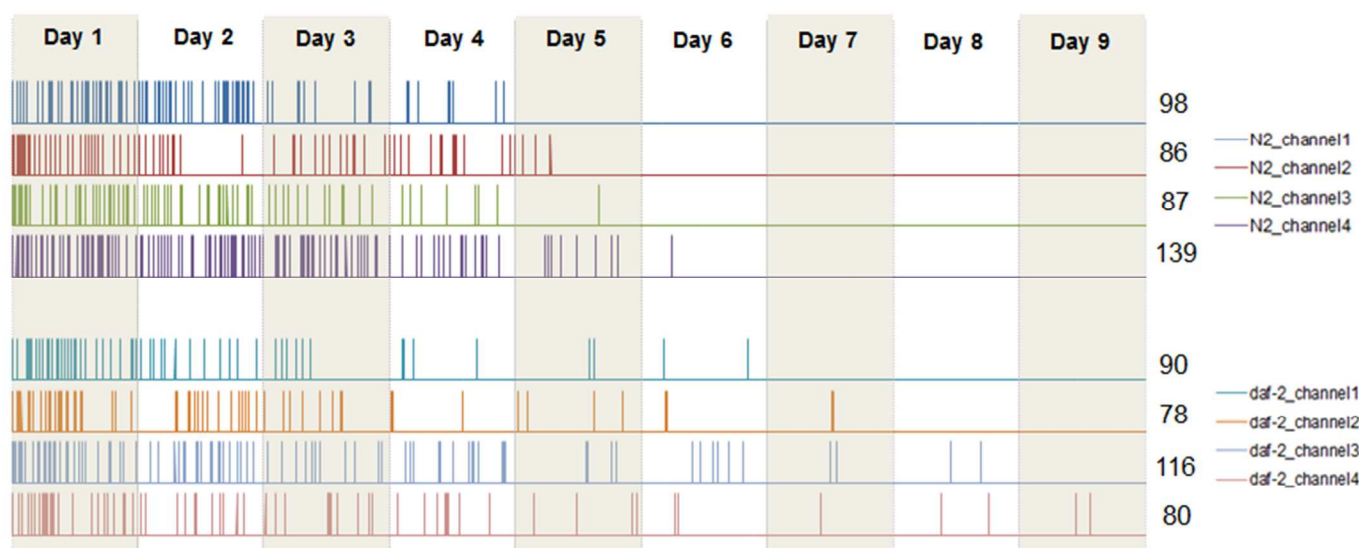
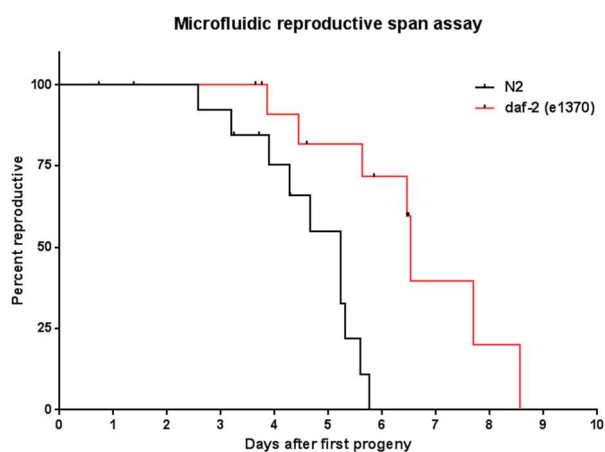


Figure 3: The worm counting algorithm. **a)** A record of the average intensity value of 8 worms in a device measured for about 6 hours. **b)** The “standard deviation” intensity of all 8 worms for the same time period in panel a. **c)** The schematic of the “standard deviation” algorithm we used. The $\text{Channel}_k(i,j)$ represents the (i,j) pixel intensity of the k -th channel (blue or black in Figure 2a), and the $\text{Background}(i,j)$ represents the (i,j) pixel intensity of the background (red in Figure 2a). **d)** An image of all 16 channels with one detected in the 7-th channel. **e)** The peak in the “standard deviation” plot representing the worm in d).

a)



b)



c)

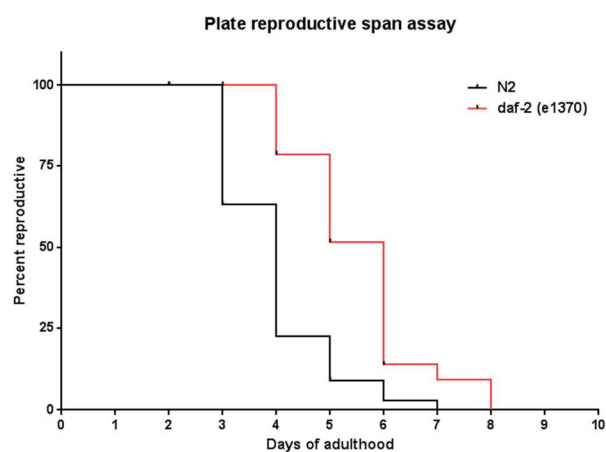


Figure 4: Time series recording of progeny production from the device. **a)** Example traces of all of the progeny production from four N2 worms and four *daf-2* mutant worms. Each peak in these traces represents signal from a single progeny. Top four data sets are from N2 worms and the bottom four data sets are from *daf-2* mutant worms. The number at the end of each trace represents the total number of the progeny from a single hermaphrodite worm over maximum of 9 days. **b)** The reproductive span curves of 13 N2 worms and 15 *daf-2* worms in two microfluidic devices. Mean RS \pm SD = 4.70 ± 0.28 days for N2,

6.63 ± 0.50 days for *daf-2*, $p = 0.001$. c) The reproductive span curve of 48 N2 worms and 48 *daf-2* worms from a conventional plate assay. The x-axis value represents the time elapsed after the first progeny of a worm. Mean RS \pm SD = 3.98 ± 0.15 days for N2, 5.52 ± 0.20 days for *daf-2*, $p < 0.0001$.

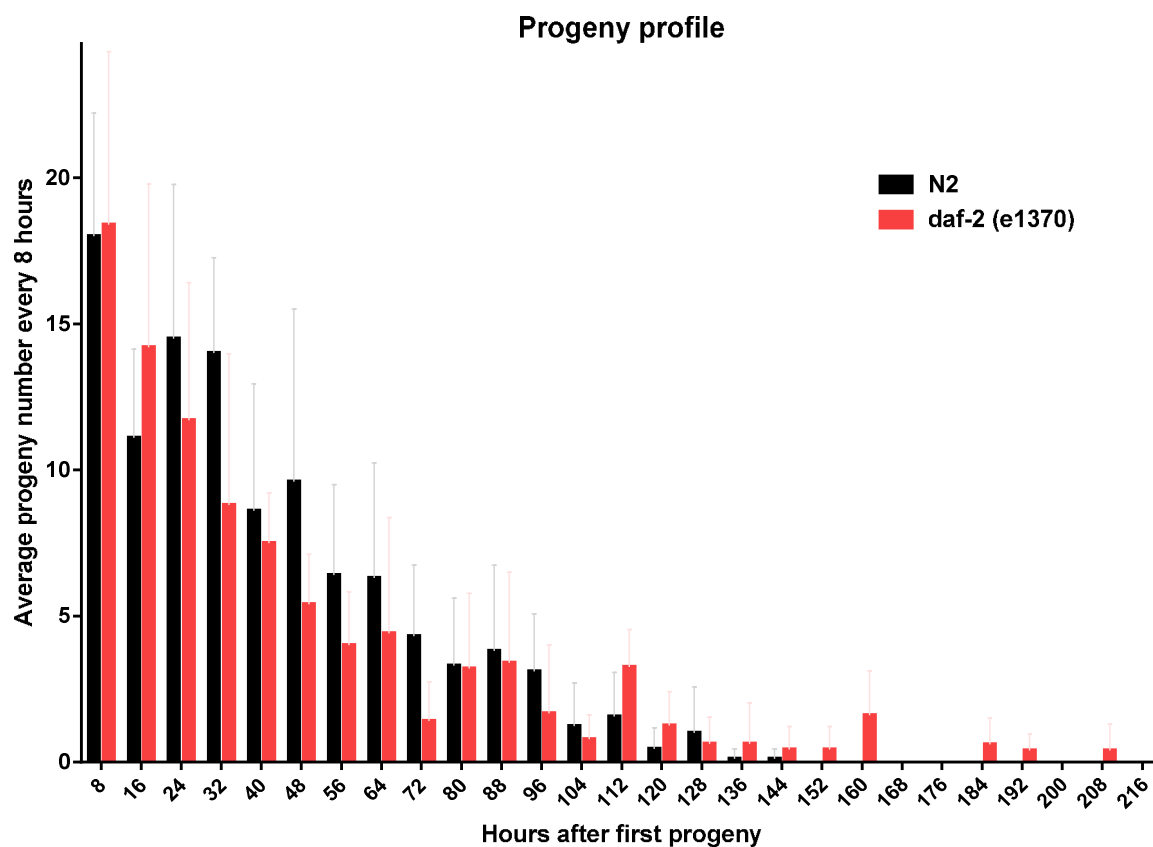


Figure 5: The average progeny number measured every 8 hours that the worms are in the experiment. The black bars and the red bars showing, respectively, the average number of progeny of 10 N2 and 10 *daf-2* worms in the microfluidic devices within the eight hour period since their first progeny were imaged.